Sampled Reference Frame Algorithm for Proposed H-Bridge Multilevel Inverter

S. Veerakumar

Abstract--- A Direct Torque Control (DTC) scheme is proposed to provide the control of the proposed inverter. There are many techniques available for DTC scheme. In this thesis DTC scheme is achieved by implementing Space Vector Pulse Width Modulation (SVPWM) technique. A Sample Reference Frame (SRF) algorithm is used to implement SVPWM and it is compared with Sector Identification (SI) algorithm, Level Shift Multi Carrier (LSMC) algorithm and Third Harmonic Reference (THR) algorithm. The SRF algorithm is implemented in this proposed work with digital controllers and it has less memory space when compared to other algorithms.

Keywords: Multi level inverter; Frame algorithm, Torque control

I. INTRODUCTION

Many control strategies are available for the control of IMs. The Direct Torque Control (DTC) is one of the most commonly used control techniques. The DTC uses SVPWM for closed loop speed control because of the high dynamic response and sinusoidal magnetic field. There are many algorithms which have been developed for SVPWM generation and three different algorithms are compared with the proposed sampled reference frame algorithm [1]. The factors like THD, Processing speed and memory usage are compared with the proposed algorithm with the other three algorithms. The sampled reference frame algorithm has been proposed in this Thesis. It is implemented in PIC16f777 controller and their performance is analyzed. Hardware has been developed and the results are compared with simulation results.

II. ADJUSTABLE DRIVE SCHEME

Adjustable speed drives are generally used in industrial applications and AC motors are mostly preferred and are widely used in pumps, fans, electrical vehicles, HVAC applications, and wind generators Bose (2002).

In 1970's DC motors were preferred for adjustable speed applications. However, it has disadvantages of more maintenance, speaking of brushes and high cost, but AC motors do not have these disadvantages [2]. Therefore, AC motor is preferred for industrial applications. Because of the development in modern power converters, it is possible to achieve better performance from AC drives when compared to that of DC.

An efficient speed control technique in AC motor is V/F control method [3]. The main goal of DTC is to provide the best performance with simple control strategy (simple algorithm, simple tuning and less control equipment).

The first vector control method was field-oriented control developed by Hasse & Blaschke in the year 1972. Another method is Feedback Linearization Control (FLC) which includes new nonlinear transformation of IM as state variables. The latest control strategies for the torque control of IM are direct torque control (DTC). This control structure was very simple and it has very good dynamic behaviour, especially in adjustable speed. In the proposed work, a fast DTC control is implemented using space vector PWM technique [4].

III. DIRECT TORQUE CONTROL SCHEME

The electromagnetic torque developed in an IM can be expressed as:

$$T_e = \frac{3P}{2}\frac{L_m}{\sigma L_s L_r}\lambda_s \lambda_r \sin\theta_T \quad (1)$$

where

The Equation (1) torque T_e can be controlled directly by controlling θ_T where θ_T is the angle between the stator flux vector and $\vec{\lambda}_s$ is the rotor flux vector.

The main variable in Direct Torque Control scheme (DTC) is the stator flux vector $\vec{\lambda}_r$. It can be found from IM model. $\vec{\lambda}_s$ relates the stator voltage vector $\vec{v}_s$. The stator flux vector $\vec{\lambda}_s$ can be written as :

$$p\vec{\lambda}_s = \vec{v}_s - R_s \vec{i}_s \quad (2)$$

In the Equation (2) shows the derivative of $\vec{\lambda}_s$ reacting by changing $\vec{v}_s$. This can be achieved by controlling reference vector $\vec{V}_{ref}$ in the space vector modulation. Figure 4.1 illustrates the overall block diagram of DTC scheme based switching vector selection logic from space vector[5]. The stator flux reference $\vec{\lambda}_s^*$ is compared with the actual flux λ_s, and the error $\Delta\lambda_s$. Similarly, reference torque T_e^* is

Revised Manuscript Received on December 08, 2018.

S. Veerakumar, Department of Electrical and Electronics Engineering, Bannari Amman Institute of Technology, Sathyamangalam, Erode Dt., Tamilnadu, India.

compared with calculated torque T_e and the difference ΔT_e is the input of torque comparator. The output of the speed and torque is compared; firing pulse is generated and then it is sent to switching logic selector, and finally the inverter switches are turned ON [6].

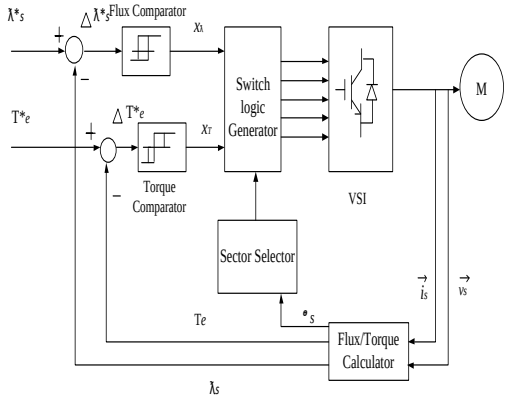

Figure 1 Block diagram of direct torque control scheme

IV. SAMPLED REFERENCE FRAME ALGORITHM

There are many algorithms that have been proposed to calculate T_1 and T_2 but all these algorithms use trigonometric functions. The trigonometric function requires more processing time during digital implementation and also requires high end DSP controllers for processing. The proposed sampled reference frame algorithm which requires less computation time and uses only arithmetic operations. The lower end 8-bit controller is sufficient to perform this task as these algorithms have reduced output THD content. This algorithm does not require sector information that reduces the memory usage in microcontrollers.[7]

This method is based on the principle of equivalence of SVPWM with sinusoidal PWM (SPWM) and can generate the SVPWM signals directly from the instantaneous reference phase voltages. In the sinusoidal PWM scheme for two-level inverters, each reference phase voltage is compared with the triangular carrier, and the individual pole voltages are generated independently of each other[8]. To obtain the maximum possible peak amplitude of the fundamental phase voltage in linear modulation, a common mode voltage V_{offset} is added to the reference phase voltages, where the magnitude of V_{offset} is given by,

$$V_{offset} = -\left(V_{max} + V_{min}\right)/2 \tag{3}$$

Where V_{max} is the maximum magnitude of the three sampled reference phase voltages, while V_{min} is the minimum magnitude of the three sampled reference phase voltages. In a sampling interval, the addition of the common mode voltage V_{offset} results in the active inverter switching vectors being centered in a sampling interval, making the SPWM technique equivalent to the SVPWM technique[9].

The Equation is based on the fact that, in a sampling interval the reference phase, which has lowest magnitude (termed the min phase) first crosses the triangular carrier and causes the first transition in the inverter switching state. When the reference phase, which has the maximum magnitude (termed the max phase) crosses the carrier last and causes the last switching transition in the inverter switching states in a two-level SVPWM scheme.[10]

Thus, the switching periods of the active vectors can be determined from the (max-phase and min phase) sampled reference phase voltage amplitudes in a two-level inverter scheme. The idea behind this SVPWM technique is to determine the sampled reference phase, from the three sampled reference phases, which crosses the triangular wave first (first-cross) and the reference phase which crosses the triangular wave last (third-cross). This SVPWM technique presents a simple way to determine the time instants at which the three reference phases cross the triangular carriers using only the instantaneous reference phase amplitudes. These time instants are sorted to find the offset voltage as illustrated in the Figure 2.

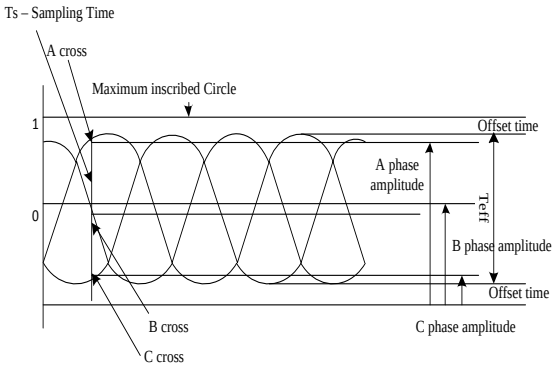

Figure 2 Instantaneous switching time calculation

The sampled voltage is added to the reference phase voltages, so the middle inverter switching vectors are centered (during a sampling interval), as in the conventional two-level SPWM scheme. The steps involved in the sampled reference frame algorithm are as follows [10].

Step1:

Find the sampled values for reference phase voltages

$$V_{as} = \sin\theta \tag{4}$$

$$V_{bs} = \sin\left(\theta + 120°\right) \tag{5}$$

$$V_{cs} = \sin\left(\theta + 240°\right) \tag{6}$$

Step2:

Find the time equivalent of each voltage

$$T_{as} = V_{as} * \left(\frac{T_S}{V_{DC}}\right) \tag{7}$$

$$T_{bs} = V_{bs} * \left(\frac{T_S}{V_{DC}}\right) \tag{8}$$

$$T_{cs} = V_{cs} * \left(\frac{T_S}{V_{DC}} \right) \quad (9)$$

where T_S is the sampling time and V_{DC} is the DC input voltage to the multilevel inverter.

Step3:

$$max\left(T_{as}, T_{bs}, T_{cs}\right) \quad (10)$$

$$min\left(T_{as}, T_{bs}, T_{cs}\right) \quad (11)$$

Step 4:

Find offset time period

$$T_{offset} = -\left(T_{max} + T_{min}\right)/2 \quad (12)$$

Step5:

Find the time period for inverter leg switches,

$$T_{ga} = T_{as} + T_{offset} \quad (13)$$

$$T_{gb} = T_{bs} + T_{offset} \quad (14)$$

$$T_{gc} = T_{cs} + T_{offset} \quad (15)$$

V. RESULTS AND DISCUSSION

Various SVPWM algorithms are simulated using MATLAB. The output waveforms of voltage, current and THD content of various algorithms are depicted.

The algorithms are listed as follows.

- Sector Identification Algorithm
- Level Shift Carrier SVPWM Algorithm
- Third Harmonic Induction Method
- Sampled Reference Frame Algorithm

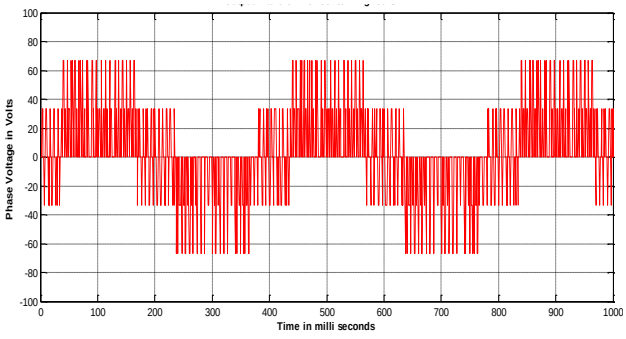

(a)

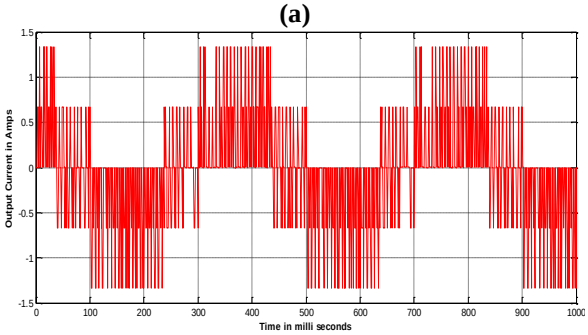

(b)

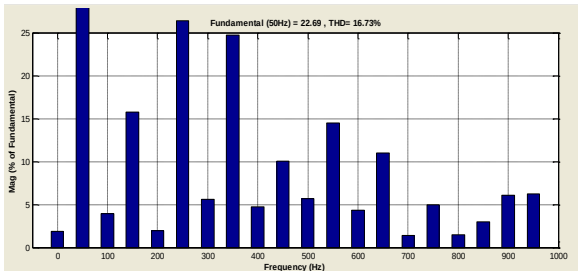

(c)

Figure 3 Output waveforms of sector identification algorithm (a) Voltage (b) Current (c) THD

Figures 3 (a), (b), and (c) show the simulated output voltage, current, and THD waveform of sector identification algorithm. The MATLAB/Simulink model has been developed for the sector identification algorithm.

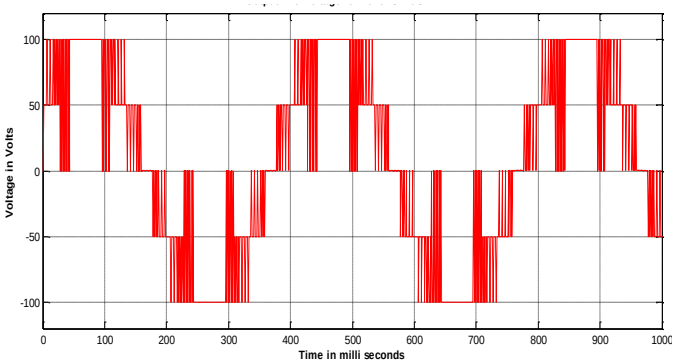

(a)

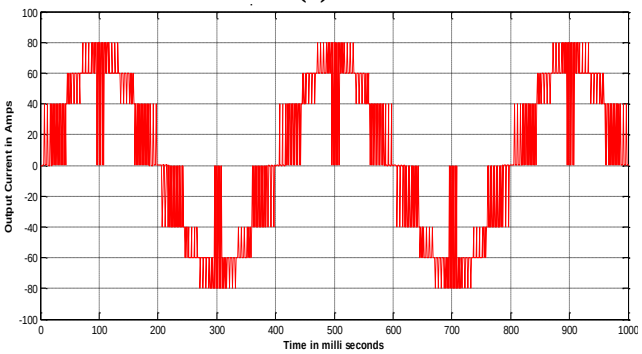

(b)

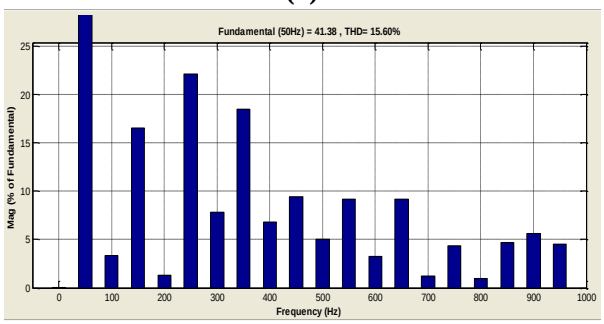

(c)

Figure 4 Output waveforms of level shift carrier (a) Voltage (b) Current (c) THD

Figures 4 (a), (b), and (c) show the simulated output voltage, current, and THD waveform of level shift SVPWM

algorithm. The MATLAB/ Simulink model has been developed for the level shift SVPWM algorithm.

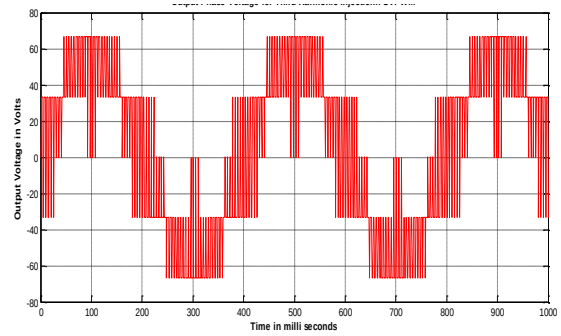

(a)

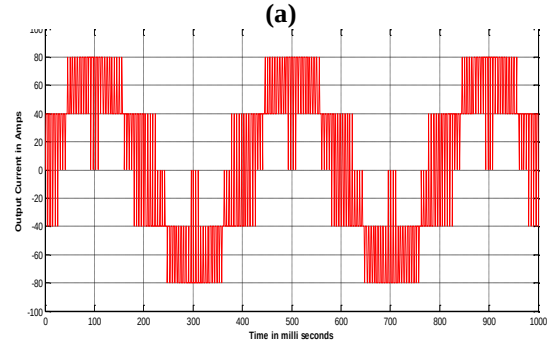

(b)

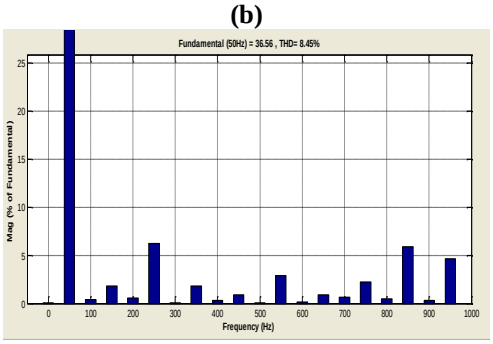

(c)

Figure 5 Output waveforms of third harmonic injection method (a) Voltage (b) Current (c) THD

Figures 5 (a), (b), and (c) show the simulated output voltage, current, and THD waveform of third harmonic injection SVPWM algorithm. The MATLAB/Simulink model has been developed for the third harmonic injection SVPWM algorithm.

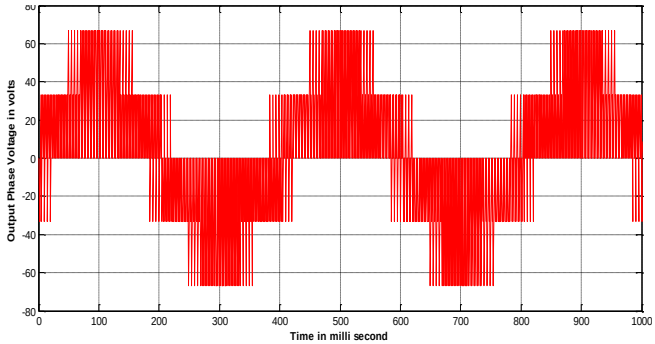

(a)

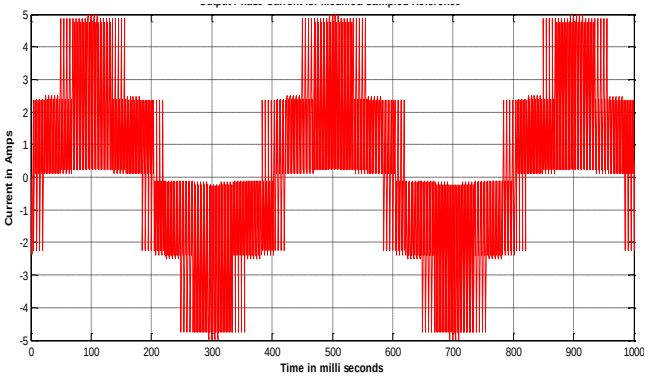

(b)

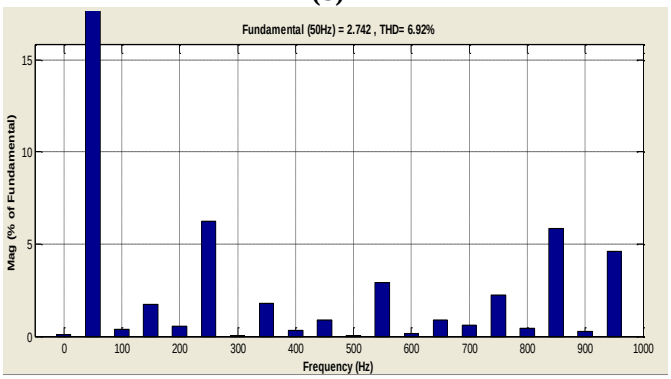

(c)

Figure 6 Output waveforms of sample reference frame algorithm (a) Voltage (b) Current (c) THD

Figures 6 (a), (b), and (c) show the simulated output voltage, current, and THD waveform of sampled reference frame SVPWM algorithm. The MATLAB/Simulink model has been developed for the sampled reference frame SVPWM algorithm.

The simulation study has been carried out using MATLAB R2010a, Pentium 5, 2 GHz, 4 GB RAM computer environment at the sampling frequency of 10 kHz. This simulation result shows that the output THD content of the sampled reference frame algorithm is less in compared to other SVPWM algorithms as shown in the Figure 7.

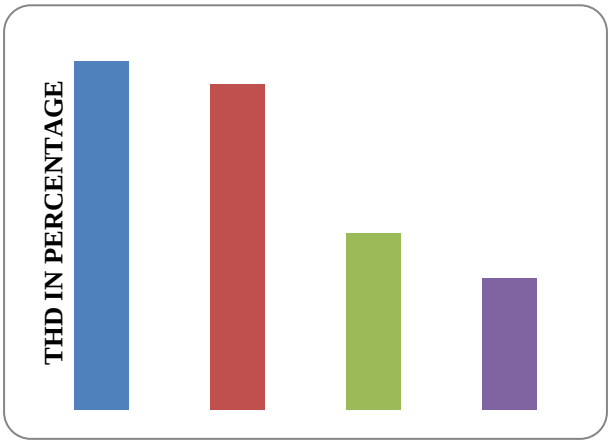

Figure 7 THD comparision of proposed and existing algorithms

Published By:
Blue Eyes Intelligence Engineering
& Sciences Publication

VI. USAGE OF MEMORY SPACE IN CONTROLLERS

The proposed sampled reference frame algorithm requires less memory space in microcontrollers. The MikroC compiler has been used to develop the algorithm in Embedded C programming. The compiler's result shows the memory usage of the proposed algorithm with sector identification algorithm. The PIC16F777 has the flash memory of 352 bits the SRF algorithm uses 17.9% of the total RAM space.

Figure 8 shows the memory usage of sector identification algorithm and memory usage of the proposed algorithm used in PIC16F777 controller. The result shows the memory usage of the proposed system is very less, hence the lower end 8-bit controller is enough to generate SVPWM.

The chart indicates the RAM used by the proposed algorithm and sector identification algorithm respectively. The result shows that the proposed system uses only 17.9% of total available RAM space in 8-bit PIC controller for arithmetic operations.

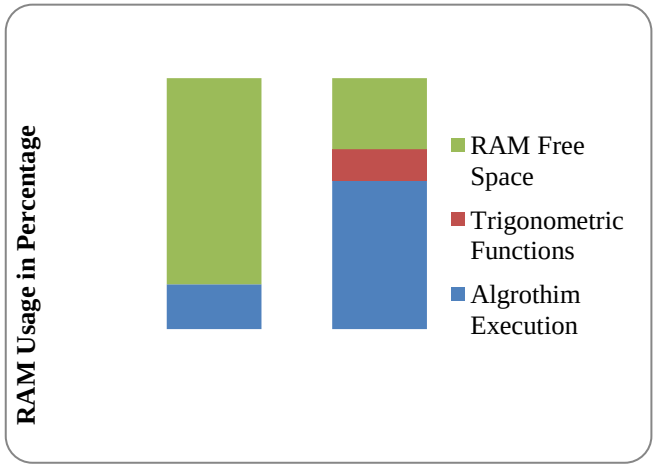

Figure 8 Comparison of RAM usage of sector identification algorithm sampled reference frame algorithm

The sector identification algorithm uses 12.5% of total available RAM space in controller is dedicated for trigonometric operation remaining 59.2% of RAM space is used for offline calculation. Moreover, in the proposed algorithm, total process is interrupt driven, so offline computation time is very less hence the controller is free to perform other operations like processing analog conversion values and calculating T_1 and T_2. However, in sector identification algorithm the total process was carried out by the main program which requires more machine cycle.

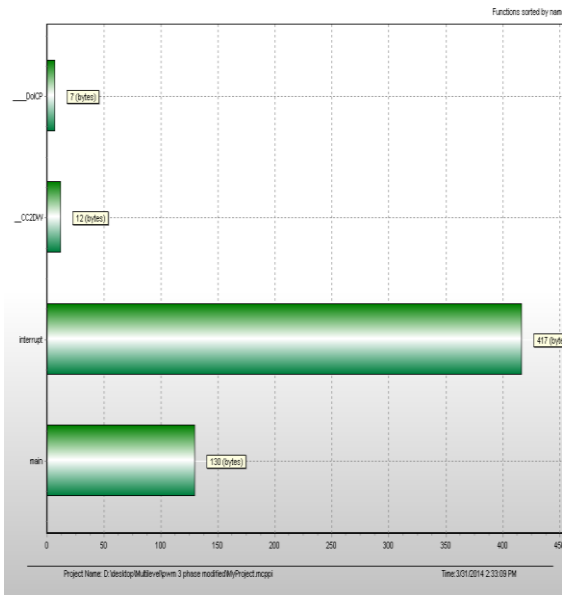

(a)

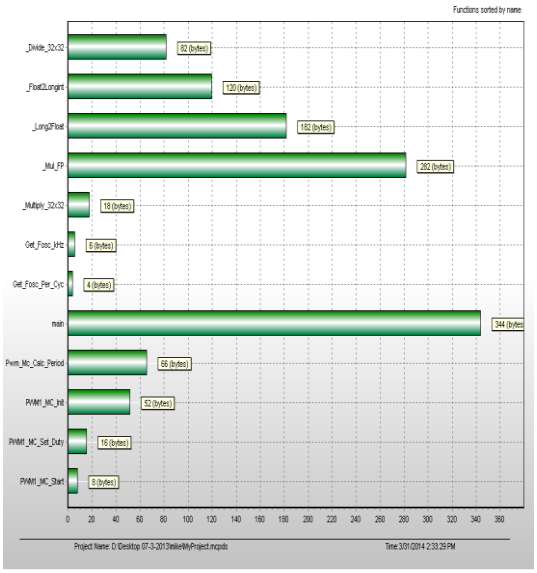

(b)

Figure 9 Processing time chart (a) Proposed SRF algorithm (b) SI algorithm

Figure 9 shows the functions required to execute the proposed SRF algorithm. It is observed that PIC requires very less functions for executing the proposed algorithm and the program is fully interrupt driven so the controller has more time for performing other operations like converting ADC values and loading PWM duty values to the duty cycles register. But in the SI algorithm the whole function is executed from the main program so controller is always busy and the functions required is more

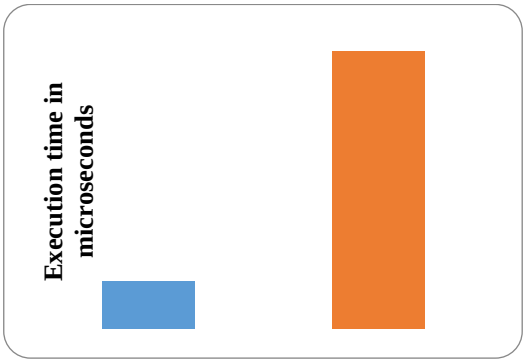

Figure 10 Comparison of algorithm execution time

The Figure 10 shows the comparison of the execution of proposed SRF algorithm and SI algorithm. The instructions required for executing SRF algorithm is 1123 instructions, SI algorithm requires 6571 only instructions. The PIC controller requires 4 clock pulse to execute one instruction for the clock frequency of 16 MHz. The time required to execute one instruction is 0.02µs. The total time required to execute SI algorithm is 22.46µs and the total time required to execute proposed algorithm is 131.42µs which requires 5 times more execution time than conventional algorithm.

The flowchart of the proposed algorithm is shown in Figure 11. In the main program, the calculation of T_{max}, T_{min} and T_{mid} for the sampled value of V_a, V_b and V_c are carried out. Figure 12 shows the Interrupt Service Routine (ISR) for Timer 1, which involves the calculation of T_{offset} and loading duty cycle values in PWM register.

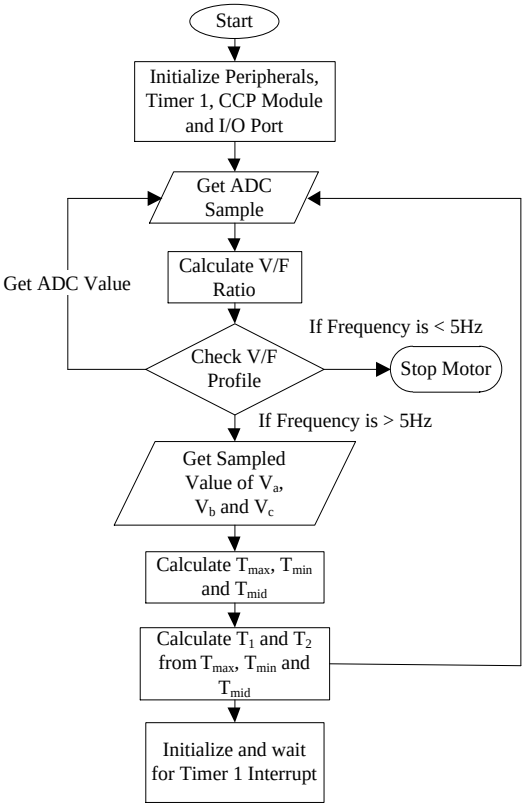

Figure 11 Flowchart for main program

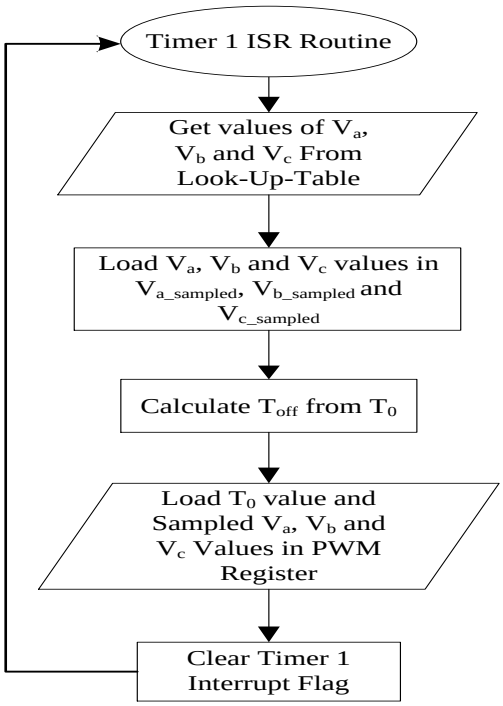

Figure 12 Timer 1 interrupt service subroutine

VII. TORQUE SPEED PERFORMANCE OF THE ELECTRIC VEHICLE

The performance of the proposed algorithm has been analyzed using MATLAB r2013a with the computer hardware environment of 1 GB of RAM, 320 GB hard disk, 2 GHz processing speed. The MATLAB Simulink model has been shown in the figure 13. The proposed algorithm has been developed using MATLAB embedded tool system tool and overall system performance has been studied and results are depicted.

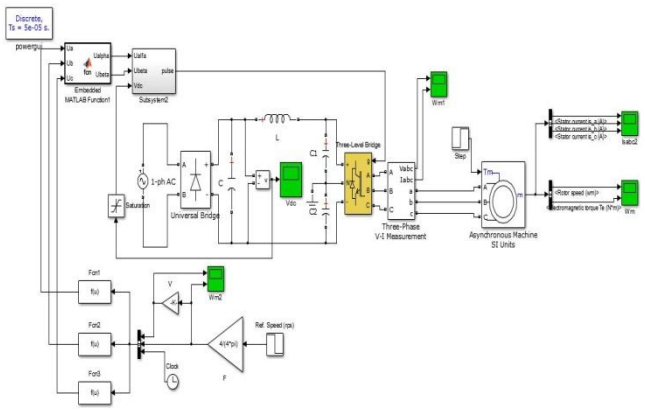

Figure 13 MATLAB Simulink model of the proposed control strategy

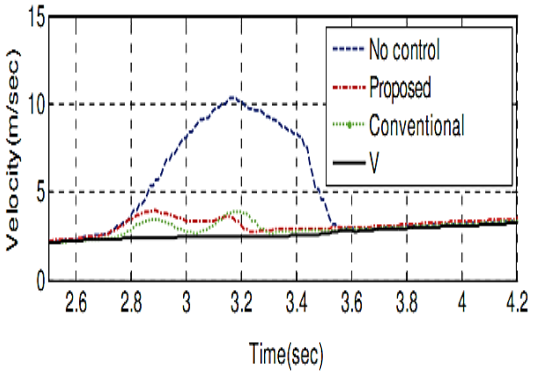

Figure 14 Velocity performances of various SVPWM algorithms

The figure 14 shows the velocity of the electric vehicle under the dynamic behaviour with the 80 % of the full load. The graph shows that without control technique, the time required for reaching the settling point is 3.5 seconds with the velocity of 10 m/sec. However conventional control strategy requires 3.3 seconds with the velocity of 4 m/sec. Proposed control system settles in 3.2 seconds with the velocity of 3 m/sec where, V is the reference velocity.

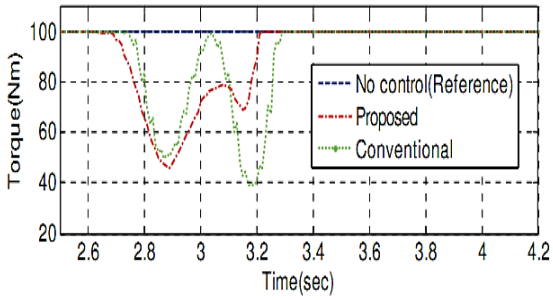

Figure 15 Torque performances of various SVPWM algorithms

The torque performance under dynamic behaviour figure 15 shows the torque fluctuation. The conventional control technique has more torque deviations during the time 2.85 Seconds the torque delivered by the control strategy was 50 Nm and at the time of 3.1 seconds it delivers the torque of 40 Nm. The conventional system delivers the torque of 50 Nm at the time of 2.85 Seconds and for the time of 3.1 Seconds it delivers the torque of 70 Nm. The conclusion is that the proposed algorithm can deliver more torque during the transient conditions.

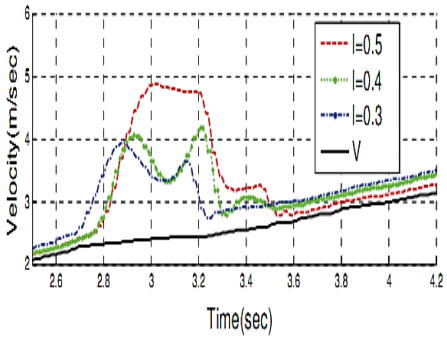

Figure 16 Velocity performances of SI algorithm for the various acceleration times

The figure 16 shows the velocity variations of the existing algorithm for the various acceleration times with increase in speed command for the time of 3 milliseconds. The vehicle reaches its stable point at the time of 3.2 seconds with the average velocity of 3.8 m/sec. Similarly, for an increase in acceleration time of 4 milliseconds, the vehicle reaches its settling point at 3.3 seconds with the average velocity of 4.1 m/sec. for the speed command of 5 milliseconds vehicle reach its settling point at 3.54 seconds with the average velocity of 5 m/sec.

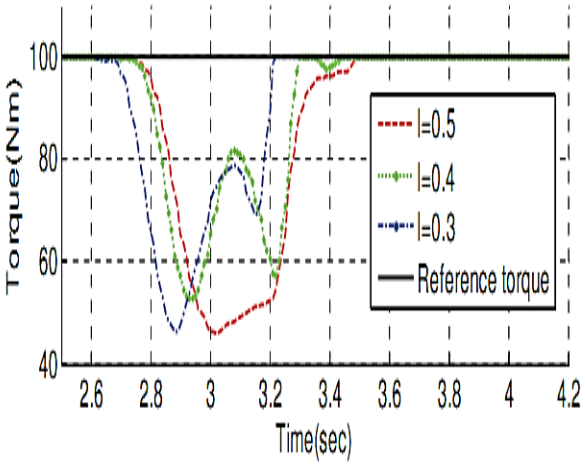

Figure 17 Torque performances of SI algorithm for the various acceleration times

The figure 17 shows the torque fluctuation of the existing algorithm for the various acceleration times for the acceleration delay of 3 milliseconds the average torque output from the vehicle is 50 Nm. Similarly, for the acceleration delay of 4 milliseconds the average output torque delivered is 60 Nm. The acceleration time of 5 milliseconds the average output torque is 50 Nm

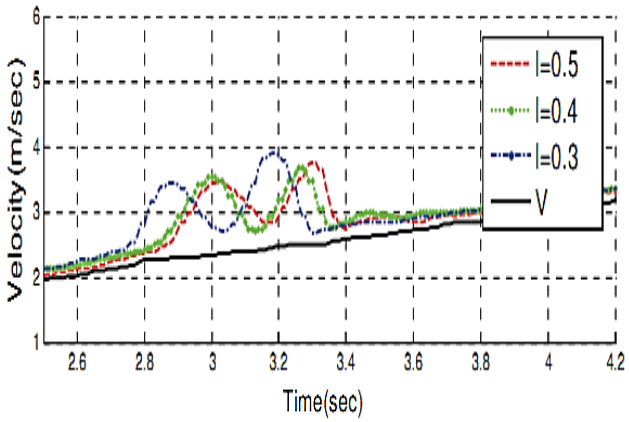

Figure 18 Velocity performances of SRF algorithm for the various acceleration times

The figure 18 shows the velocity variations of the proposed algorithm for the various acceleration times with increase in speed command for the time of 3 milliseconds. The vehicle reaches its stable point at the time of 3.3 seconds with the velocity of 3.5 m/sec. Similarly, increase in

acceleration for the time of 4 milliseconds the vehicle reach its settling point at 3.45 seconds with the velocity of 3.6 m/sec. for the speed command of 5 milliseconds vehicle reach its settling point at 3.4 seconds with the average velocity of 3.9 m/sec.

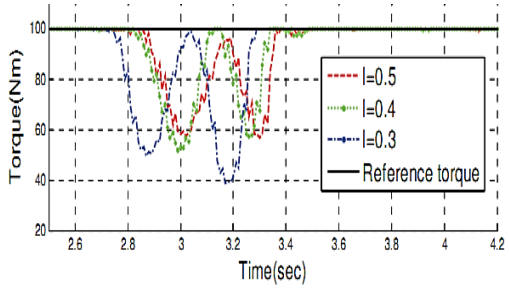

Figure 19 Torque performances of SRF algorithm for the various acceleration times

The figure 19 shows the torque fluctuation for the various acceleration times for the acceleration delay of 3 milliseconds the average torque output from the vehicle is 40 Nm. Similarly, for the acceleration delay of 4 milliseconds the average output torque delivered is 50 Nm. The acceleration time of 5 milliseconds the average output torque is 45 Nm.

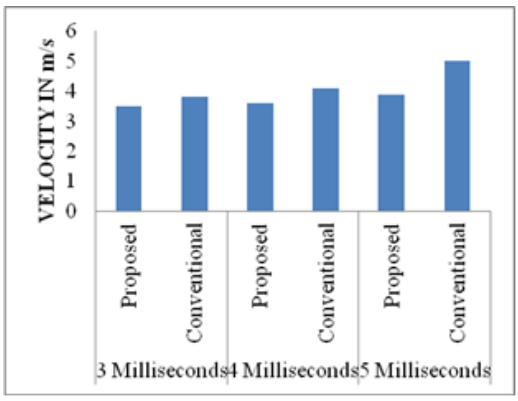

Figure 20 Velocity comparison of various acceleration times

The figure 20 shows the overall performance in electric vehicle for the velocity with the various acceleration time. The results clearly show that proposed SRF algorithm reacts quickly and reach its equilibrium point in comparison to the Sector Identification algorithm.

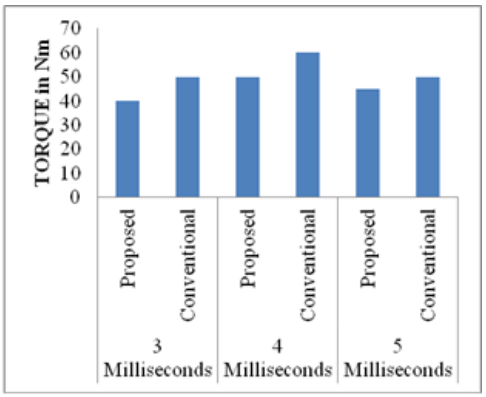

Figure 21 Torque comparison of various acceleration times

Similarly figure 21 shows the torque developed in the proposed algorithm is less, because the velocity developed during transient conduction is less. So the proposed algorithm requires less torque during acceleration so the current consumed by the overall system is within the maximum allowable limit.

The sampled reference frame algorithm is implemented in the lower end controller and its performance analysis has been carried out. This controller has 3 CCP modules, but for five-level inverter 12 PWM channels are required. This can be obtained from the logical switching selector. The input and output port of PIC microcontroller is configured to generate the logical switching pulse. The logical switching sector signal has given to the logic gates for generating five level PWM.

Figure 2 shows the SVPWM output from the CCP pin for R Phase and Y Phase. Digital Storage Oscilloscope (DSO) captures the output pulses. The frequencies of SVPWM are generated at 16 kHz. Figure 23 shows the switching logic selection pulse and PWM pulses for the R Phase High side MOSFET's. Figure 24 shows the two switching logic selector signal for VSI and H Bridge inverters. The logical pulse is given to logical switching selector.

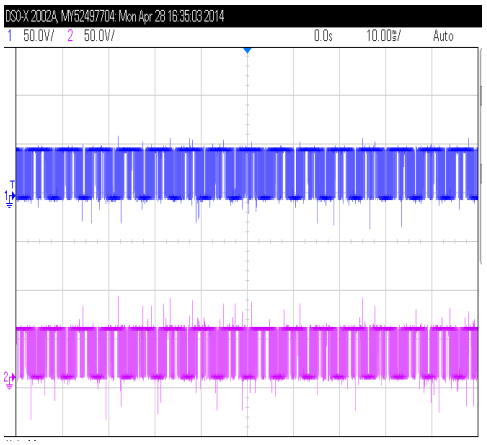

Figure 22 R Phase and Y Phase SVPWM from CCP Module

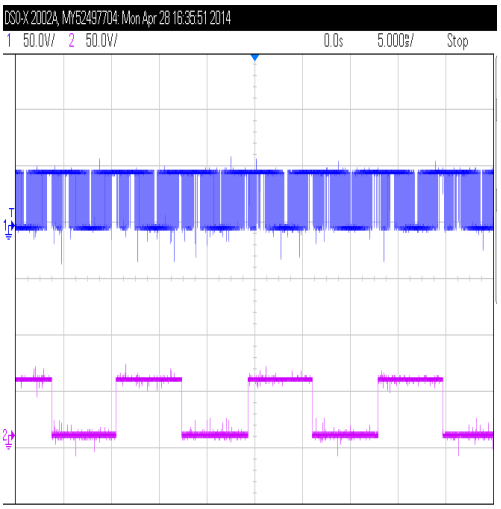

Figure 23 SVPWM and switching logic pulse

Published By:
Blue Eyes Intelligence Engineering
& Sciences Publication

The logical selector output of the proposed five-level inverter is shown in Figure 25. The Figure 26 shows the upper PWM pulses, which are given to the H-Bridge, and lower PWM pulses are given to the VSI inverter switches.

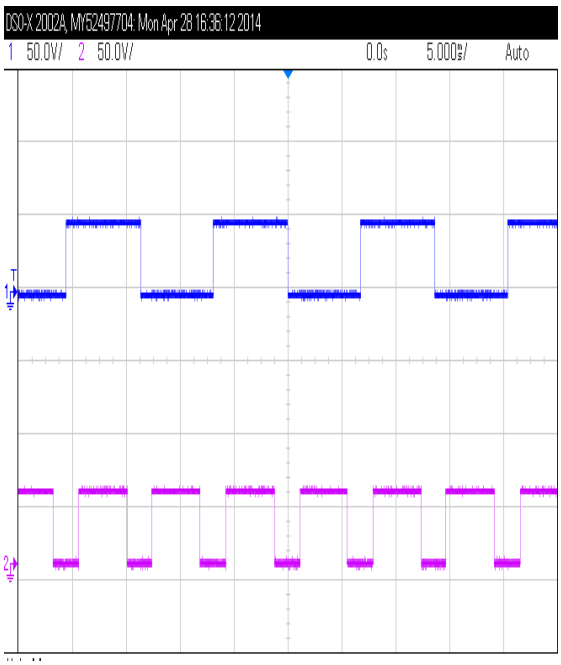

Figure 24 Switching logic selector pulse

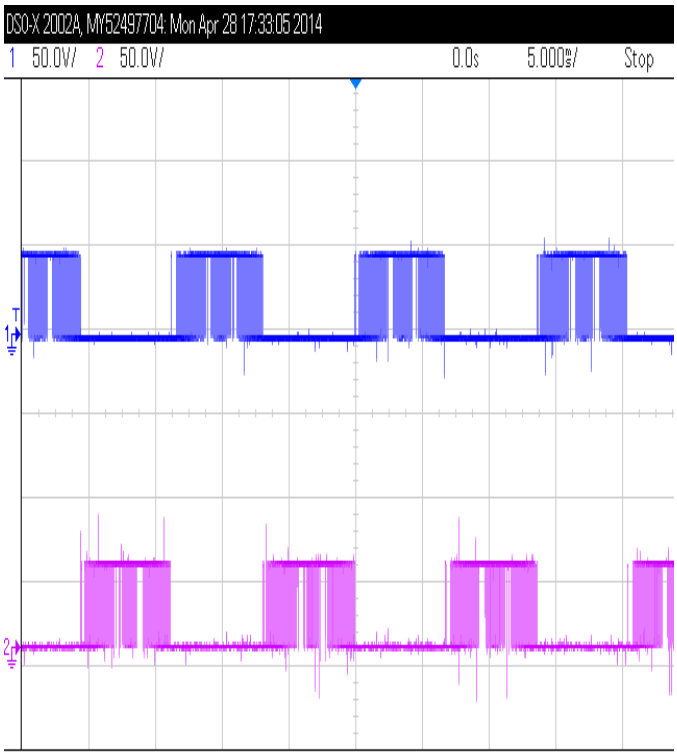

Figure 25 Positive and negative gating signals to VSI

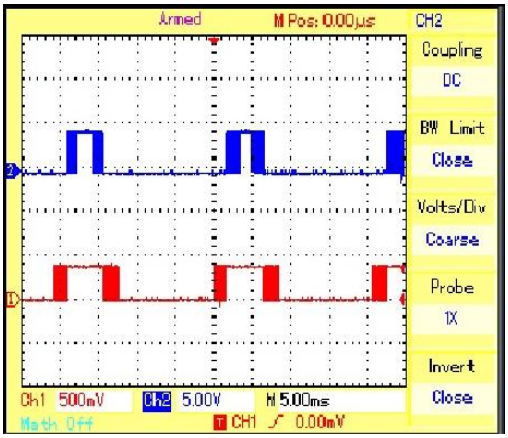

Figure 26 Gating pulse for VSI and H-Bridge inverter

Figure 27 shows the gating pulse of positive and negative H Bridge switches. The PWM output from the logical switching selector is given to TLP250 OPTO isolated driver. The amplified signal is given to MOSFET gates. Figure 28 shows the amplified output waveform of high side and low side pulses.

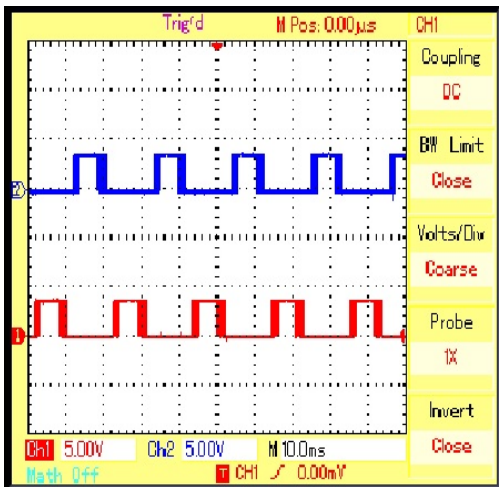

Figure 27 Positive and negative gating pulses to H-Bridge

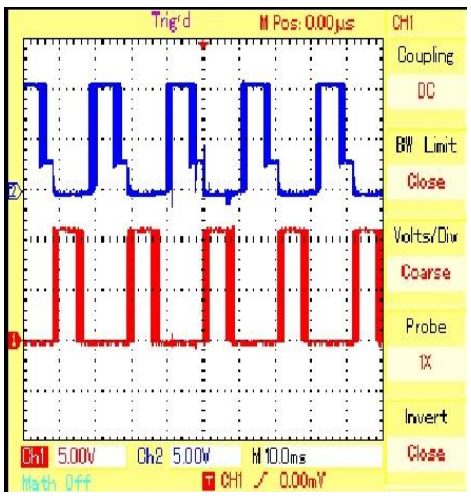

Figure 28 TLP250 boost strip output to MOSFET

Published By:
Blue Eyes Intelligence Engineering
& Sciences Publication

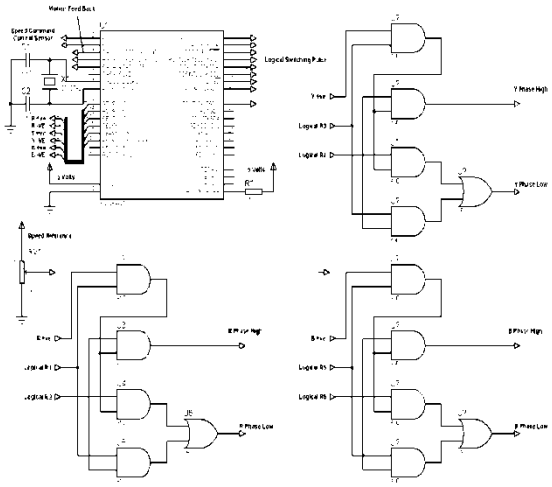

Figure 29 Circuit diagram of microcontroller and switching logic selector

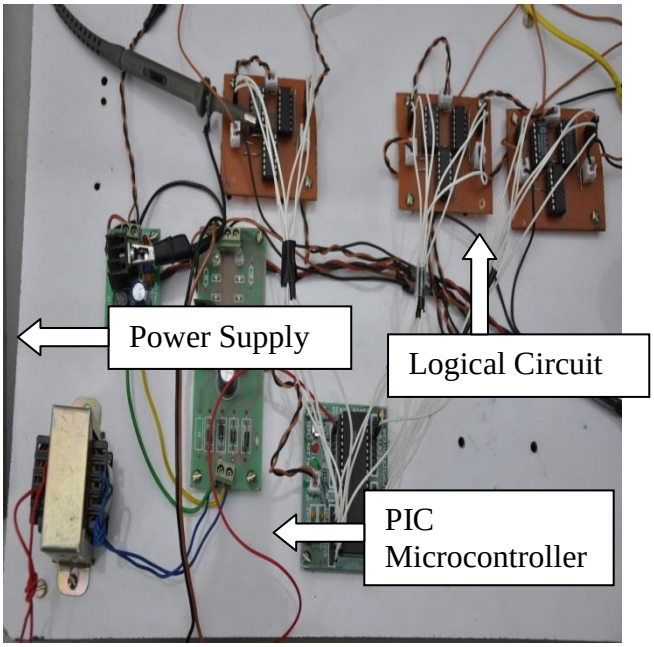

Figure 30 Proposed Hardware modules of microcontroller and switching logic selector

Figure 29 shows the circuit diagram of PIC16F777 and switching logic selector for generating logical pulse. The logical pulses are fed to the TLP250 OPTO coupler and finally given to the MOSFET. The switching logic selector has the AND gate and NAND gate to produce the positive and negative gating pulse. Figure 30 shows the PIC microcontroller and logical switching selector circuits. The operating frequency of PIC microcontroller is 16 MHz and the logical switching selector circuit is implemented using the IC's, IC 7804 and IC 7812 and it is used to generate the five-level PWM pulse.

VIII. CONCLUSION

The various SVPWM algorithms have been investigated based on execution time, usage of memory space in controllers with reduced output voltage THD. The proposed sampled reference frame algorithm has been compared with the conventional sector identification algorithm based on the above mentioned factors. The proposed algorithm occupies less space in controllers; moreover it does not requires trigonometric functions which results in reduced offline computation time. This algorithm has been implemented in PIC16F777 microcontroller and the results are validated.

REFERENCE

1. Wan Noraishah Wan Abdul Munim, Mohd Firdaus Ismail, Ahmad Farid Abidin "Switching technique comparison for multi-phase inverters", 2013 IEEE 7th International Power Engineering and Optimization Conference (PEOCO2013), Langkawi, Malaysia. 3-4 June 2013.
2. P. S. N. de Silva, J. E. Fletcher, and B. W. Williams, "Development of space vector modulation strategies for five phase voltage source inverters," in Power Electronics, Machines and Drives, 2004. (PEMD 2004). Second International Conference on (Conf. Publ. No. 498), 2004, pp. 650-655 Vol.2.
3. R. Hyung-Min, K. Jang-Hwan, and S. Seung-Ki, "Analysis of multiphase space vector pulse-width modulation based on multiple d-q spaces concept," Power Electronics, IEEE Transactions on, vol. 20, pp. 1364-1371, 2005.
4. B. Wu, High Power Converters and AC Drives New Jersey: IEEE Press, 2006.
5. Jay K. Pandit, MohanV.Aware, Ronak V. Nemade, Emil Levi, "Direct Torque Control Scheme for a Six-Phase Induction Motor With Reduced Torque Ripple", IEEE TRANSACTIONS ON POWER ELECTRONICS, VOL. 32, NO. 9, SEPTEMBER 2017
6. Levi, R. Bojoi, F. Profumo, H. Toliyat, and S. Williamson, "Multiphase induction motor drives—A technology status review," IET Elect. Power Appl., vol. 1, no. 4, pp. 489–516, Jul. 2007.
7. Gomathi C, Navya Nagath, Veerakumar S," Sampled Reference Frame Algorithm Based on Space Vector Pulse Width Modulation for Five Level Cascaded H-Bridge Inverter" Buletin Teknik Elektro dan Informatika (Bulletin of Electrical Engineering and Informatics) Vol. 3, No. 2, June 2014, pp. 127~140 ISSN: 2089-3191
8. Pablo Lezana, José Rodriguez, and Diego A Oyaizu, "Cascaded Multilevel Inverter With Regeneration Capability and Reduced Number of Switches". IEEE Trans. On Industrial Electronics. 2008; 55(3): 1059-1066.
9. Adam GP, O Anaya-Lara, GM Burt, D Telford, BW Williams, and JR McDonald. "Modular multilevel inverter: pulse width modulation and capacitor balancing technique". Published in IET Power Electronics. 2010; 3(5): 702-715.
10. Mohan M Renge and Hiralal M Suryawanshi. "Three-Dimensional Space-Vector Modulation to Reduce Common-Mode Voltage for Multilevel Inverter". IEEE Trans. On Industrial Electronics 2010; 57(7): 2324-2331.